DOI:10.1093/jnci/djt263
Advance Access publication October 3, 2013

ARTICLE

Combating Resistance to Anti-IGFR Antibody by Targeting the Integrin β3-Src Pathway

Dong Hoon Shin, Hyo-Jong Lee, Hye-Young Min, Sun Phil Choi, Mi-Sook Lee, Jung Weon Lee, Faye M. Johnson, Kapil Mehta, Scott M. Lippman, Bonnie S. Glisson, Ho-Young Lee

Manuscript received April 16, 2013; revised August 15, 2013; accepted August 20, 2013.

Correspondence to: Ho-Young Lee, PhD, College of Pharmacy and Research Institute of Pharmaceutical Sciences, Seoul National University, 1 Gwanak-ro, Gwanak-gu, Seoul 151–742, Republic of Korea (e-mail: hylee135@snu.ac.kr).

Background Several phase II/III trials of anti–insulin-like growth factor 1 receptor (IGF-1R) monoclonal antibodies (mAbs) have shown limited efficacy. The mechanisms of resistance to IGF-1R mAb-based therapies and clinically applicable strategies for overcoming drug resistance are still undefined.

Methods IGF-1R mAb cixutumumab efficacy, alone or in combination with Src inhibitors, was evaluated in 10 human head and neck squamous cell carcinoma (HNSCC) and six non–small cell lung cancer (NSCLC) cell lines in vitro in two- or three-dimensional culture systems and in vivo in cell line– or patient-derived xenograft tumors in athymic nude mice (n = 6–9 per group). Cixutumumab-induced changes in cell signaling and IGF-1 binding to integrin β3 were determined by Western or ligand blotting, immunoprecipitation, immunofluorescence, and cell adhesion analyses and enzyme-linked immunosorbent assay. Data were analyzed by the two-sided Student *t* test or one-way analysis of variance.

Results Integrin β3–Src signaling cascade was activated by IGF-1 in HNSCC and NSCLC cells, when IGF-1 binding to IGF-1R was hampered by cixutumumab, resulting in Akt activation and cixutumumab resistance. Targeting integrin β3 or Src enhanced antitumor activity of cixutumumab in multiple cixutumumab-resistant cell lines and patient-derived tumors in vitro and in vivo. Mean tumor volume of mice cotreated with cixutumumab and integrin β3 siRNA was 133.7 mm^3 (95% confidence interval [CI] = 57.6 to 209.8 mm^3) compared with those treated with cixutumumab (1472.5 mm^3; 95% CI = 1150.7 to 1794.3 mm^3; $P < .001$) or integrin β3 siRNA (903.2 mm^3; 95% CI = 636.1 to 1170.3 mm^3; $P < .001$) alone.

Conclusions Increased Src activation through integrin αvβ3 confers considerable resistance against anti–IGF-1R mAb-based therapies in HNSCC and NSCLC cells. Dual targeting of the IGF-1R pathway and collateral integrin β3–Src signaling module may override this resistance.

J Natl Cancer Inst;2013;105:1558–1570

The insulin-like growth factor (IGF) axis, regulated by receptors (IGF-1R and IGF-2R), ligands (IGF-1, IGF-2, and insulin), and IGF-binding proteins, is critically important for numerous hallmarks of neoplasia (1,2), and thus is recognized as an attractive target for anticancer therapies. A number of clinical trials are under way to test two major anti–IGF-1R strategies, including monoclonal antibodies (mAbs) and tyrosine kinase inhibitors (TKIs) (3,4). Although a small subset of patients enrolled in phase I and II clinical trials demonstrated sporadic tumor responses to anti–IGF-1R mAbs (5–9), the anticancer effects have been very modest and unsustained when used alone (10–12). However, the mechanisms mediating resistance to anti–IGF-1R strategies are poorly understood.

Integrins, a family of adhesive receptors composed of 8β and 18α subunits (13) activated by ligand occupancy, induce focal adhesion kinase (FAK) autophosphorylation at tyrosine 397 (Y397), which is required for p85 binding and PI3K activation (14), the recruitment of Src, and Src-dependent phosphorylation of FAK and epidermal growth factor receptor (EGFR) (13,15). Several reports have demonstrated the implications of integrin αvβ3 in key aspects of neoplasia and antineoplastic drug resistance (16,17). Of note, a recent report showed that IGF-1 directly binds to integrin β3, but not integrin β1 (18), suggesting a direct regulatory link between the IGF system and specific integrin signals.

In this study, we sought to determine the mechanisms mediating resistance to cixutumumab (IMC-A12), a fully humanized anti–IGF-1R mAb that has been evaluated in several clinical trials (19), and to discover alternative strategies for targeting of IGF-1R and other signaling molecules involved in anti–IGF-1R mAb resistance.

Methods

Further details for some experimental procedures are described in the Supplementary Methods (available online). Reagents, preparation of poly-(HEMA [poly-2-hydroxyethyl methacrylate])-coated plates (PCPs), cell proliferation/viability and anchorage-independent colony formation assays, Western blot and enzyme-linked immunosorbent assay (ELISA), preparation of paraffin-embedded cell blocks and immunofluorescence, extracellular matrix adhesion and immunofluorescence, mouse studies, and liposomal preparation are only described online.

Cell Culture, In Vivo Experiments, and Analyses of Proliferation/Viability

All cell lines were authenticated/validated. Cells were cultured in DMEM or RPMI 1640 supplemented with 10% fetal bovine serum (FBS) and antibiotics. Cells were maintained at 37°C in a humidified atmosphere with 5% CO_2 and subcultured twice a week. Athymic nude mice were purchased from Harlan Sprague Dawley (Indianapolis, IN). The use of tissue specimens of primary head and neck squamous cell carcinoma (HNSCC) obtained from patients who had surgical resection at MD Anderson Cancer Center was approved by the Institutional Review Board, which waived the need for written informed consent. Human HNSCC and non–small cell lung cancer (NSCLC) cell culture and analyses of cell proliferation/viability under the 3D-mimic and 3D culture conditions were performed as described previously (20). Further details are described in the Supplementary Methods (available online).

Mouse Studies

All mouse study procedures were performed in accordance with protocols approved by the Institutional Animal Care and Use Committee of Seoul National University or MD Anderson Cancer Center. Mice were cared for in accordance with guidelines set by the Association for Assessment and Accreditation of Laboratory Animal Care and the US Public Health Service Policy on Human Care and Use of Laboratory Animals. For 686LN, UMNSCC38, H226B, or A549m xenograft tumors, cancer cells (1×10^6 cells/mouse in 100 µL of phosphate-buffered saline) were subcutaneously injected into nude mice at a single dorsal flank site (6–9 mice per group). For HNSCC patient–derived xenograft tumors, primary human tumor specimens were collected from an untreated patient who underwent lobectomies of squamous carcinoma of the oral cavity. Primary tumor specimens were provided by Dr. Faye M. Johnson. Further details are in Supplementary Methods (available online).

Statistical Analyses

The data acquired from in vitro assays were analyzed by Student *t* tests. All sample means and 95% confidence intervals from multiple samples (n = 5–8) were calculated using Microsoft Excel 2007 software (Microsoft Corporation, Redmond, WA). The statistical significance of differences in tumor growth in the combination treatment group and in the single-agent treatment group was analyzed using the one-way analysis of variance (IBM SPSS version 21, Armonk, NY). In all statistical analyses, two-sided *P* values of less than .05 were considered statistically significant.

Results

Effect of Cixutumumab on Growth of NSCLC and HNSCC Cells Under Reduced Cell Adhesion and Anchorage-Independent Culture Conditions In Vitro and In Vivo

We tested the effects of 25 µg/mL cixutumumab, which almost completely suppressed IGF-1–induced IGF-1R phosphorylation (Supplementary Figure 1, available online), on a panel of 13 HNSCC and 6 NSCLC cell lines grown in poly-2-hydroxyethyl methacrylate (polyHEMA)–coated plates (PCPs) and in ultra-low attached plates (UAPs) (21). These cells formed spheroidal cell masses and grew for at least 7 days in the 3D-mimic conditions (Supplementary Figure 2A, available online). Cixutumumab-treated OSC19 cells had substantially slower growth rates than did untreated cells, whereas 686LN and FADU cells showed no detectable difference after the drug treatment (Supplementary Figure 2B, available online). We have previously reported the effects of cixutumumab on the proliferation of these cell lines grown in PCPs and UAPs for 3 days (20). Because cancer cells grown in 3D-mimetic systems might differ from those grown in tumors under the 3D condition, in this study, we analyzed the drug response in a 3D culture condition (soft agar) as well as in PCPs and UAPs after 7–14 days of treatment. Consistent with the previous results, 7 HNSCC and 2 NSCLC cell lines grown in PCPs (Supplementary Figure 3A, available online) and UAPs (Supplementary Figure 3B, available online) experienced less than 20% inhibition in viability (defined as "resistant"); 4 HNSCC and 2 NSCLC cell lines experienced 20%–50% inhibition in viability (defined as "moderate"); and the remaining 2 HNSCC and 2 NSCLC cell lines experienced more than 60% inhibition in viability (defined as "sensitive") after cixutumumab treatment. All of the "sensitive" sublines also formed statistically significantly fewer colonies in soft agar than did "resistant" and "moderate" sublines after the drug treatment (percentage of inhibition: 28.1% ± 11.7% at 5 µg/mL, 95% confidence interval [CI] = 16.6% to 39.6%, $P < .001$; 20.3% ± 6.1% at 10 µg/mL, 95% CI = 14.3% to 26.3%, $P < .001$; 13.5% ± 5.4% at 25 µg/mL, 95% CI = 8.2% to 18.8%, $P < .001$) (Figure 1A). None of these cells under these culture conditions showed statistically significant decrease in proliferation after treatment with 25 µg/mL IgG (data not shown). Upon cixutumumab treatment, the volumes of the drug-sensitive UMSCC38 (1012.4 mm^3; 95% CI = 850.1 to 1174.8 mm^3) and A549m (454.1 mm^3; 95% CI = 212.2 to 696.0 mm^3; $P < .01$) xenograft tumors were statistically significantly smaller compared to control groups (UMSCC38, 1759.9 mm^3; 95% CI = 1626.9 to 1893.0 mm^3; $P < .01$ and A549m, 1290.0 mm^3; 95% CI = 1019.5 to 1560.6 mm^3; $P < .01$). In contrast, the growth of drug-resistant 686LN and H226B tumors were not affected (Figure 1B and Supplementary Figure 4, available online).

Association Between Cixutumumab-Induced pAkt Levels and Cixutumumab Resistance

We investigated the mechanisms of cixutumumab resistance. Consistent with our previous observations (20), cixutumumab treatment resulted in decreases in IGF-1R phosphorylation and expressions in both cixutumumab-resistant 686LN and cixutumumab-sensitive OSC19 cells grown in PCPs, UAPs, and in soft agar (Figure 2A). However, Akt dephosphorylation was observed

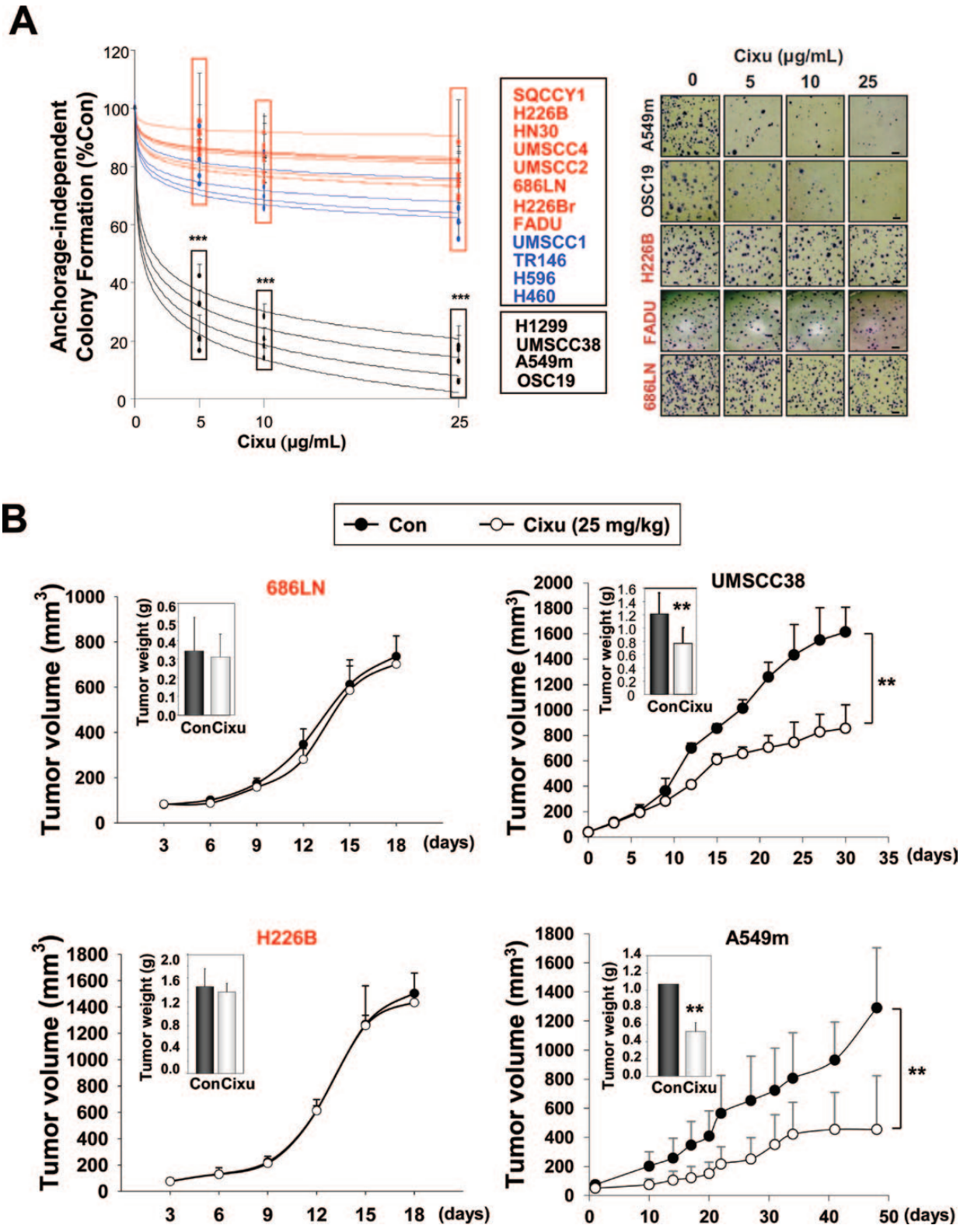

Figure 1. Differential responses of head and neck squamous cell carcinoma (HNSCC) and non–small cell lung cancer (NSCLC) cells after treatment with cixutumumab in various culture conditions in vitro and in vivo. **A**) HNSCC and NSCLC cells were cultured in soft agar for 2–6 weeks in the presence or absence of cixutumumab (0, 5, 10, or 25 μg/mL). Each bar represents the mean ± SD of three identical wells of a single representative experiment (**left**). Representative images of colony formation (**right**). (scale bar: 20 μm) **B**) Preestablished xenografts (n = 9) of indicated cells were treated with cixutumumab (Cixu; intraperitoneal; 25 mg/kg, twice a week) or vehicle (Control). Data are presented as mean tumor volume ± SD for indicated time or weight at the date of euthanasia (**inset**) ± SD. $^{**}P < .01$, $^{***}P < .001$ by two-sided Student *t* test. Cixu = cixutumumab; Con = control.

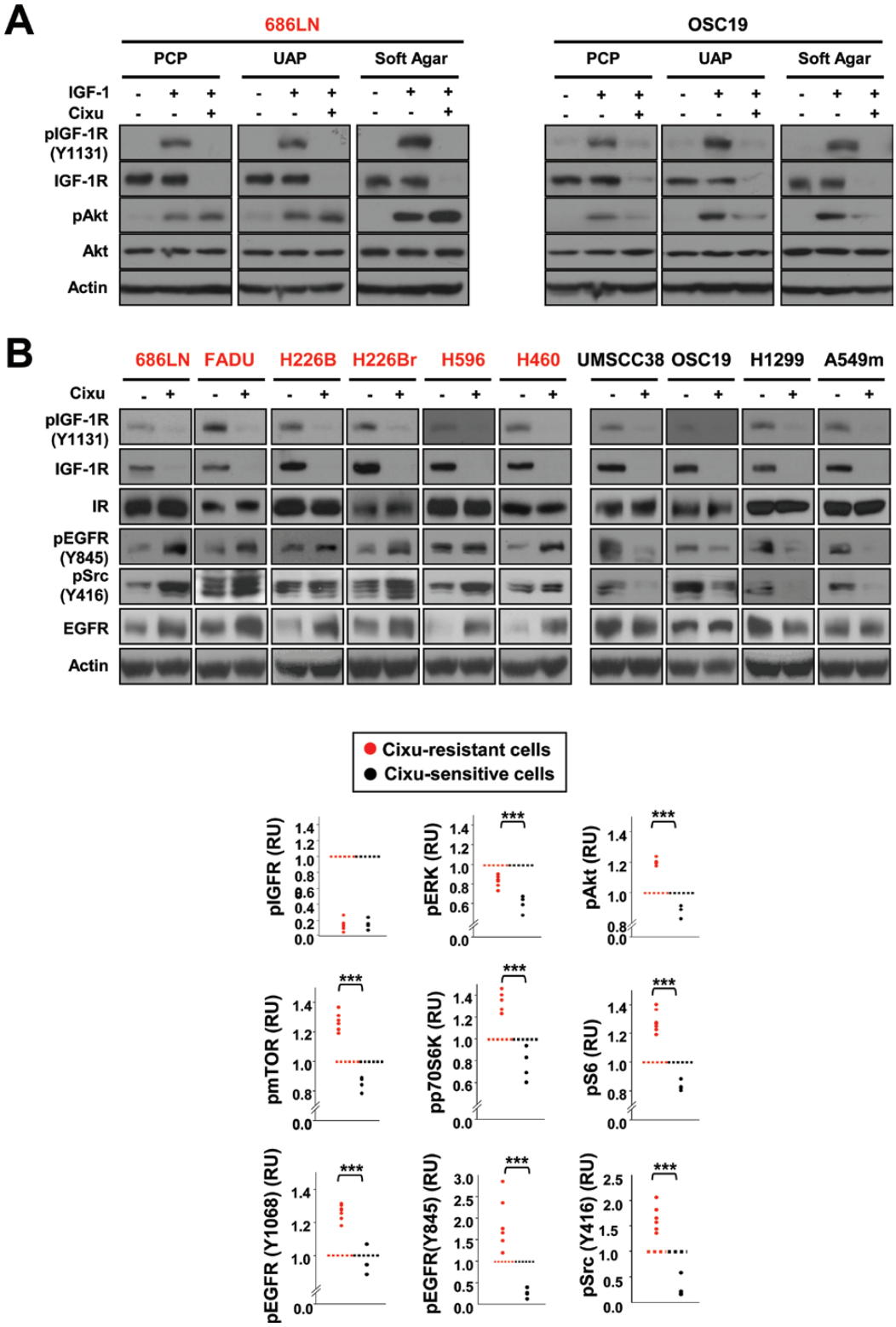

Figure 2. Characterization of signaling components involved in resistance to cixutumumab. Cixutumumab-resistant (686LN, FADU, 226B, 226Br, H596, and H460) and -sensitive (UMSCC38, OSC19, H1299, and A549m) lines grown in poly-(HEMA [poly-2-hydroxyethyl methacrylate])-coated plates (PCPs) (**A, B**), ultra-low attached plates (UAPs) (**A**), or in soft agar (**A**) were untreated (–) or treated with cixutumumab (25 μg/mL) for 6 hours (**A**) or 7 days (**B**) and then unstimulated or stimulated with insulin-like growth factor I (IGF-1) (**A**) or 10% fetal bovine serum (**B**) for 30 minutes. Indicated proteins were analyzed by Western blot analysis. Human IgG1 treatment did not affect the expression of these proteins (data not shown). Densitometric analysis (**B, bottom**) was performed to quantify the expression levels of the indicated proteins. The expression levels of the indicated proteins was calculated by using the equation [relative unit (RU) = A/C], where A and C represent the density of the indicated protein bands in cixutumumab-treated cells and vehicle-treated control cells, respectively. A representative data set from at least two independent experiments is shown. Statistical significance of differences between cixutumumab-resistant (n = 6) and -sensitive (n = 4) cells was determined by two-sided Student *t* test. ***$P < .01$. Cixu = cixutumumab.

only in OSC19 cells, but not in 686LN cells. Obviously increased phosphorylations of EGFR, Akt, and its downstream effectors, including mTOR, p70S6K, and S6, were also observed in the cixutumumab-resistant lines, but not in the sensitive lines (Supplementary Figure 5, available online). Previous findings implicated insulin receptor (IR), platelet-derived growth factor receptor (PDGFR), or AXL receptor tyrosine kinase (AXL) expression and cross-talk between EGFR and IGF-1R signaling pathways in the resistance to the IGF-1R targeting agents (22–25). However, there was no obvious association between cixutumumab sensitivity and expression of these molecules (data not shown). Of note, cixutumumab treatment increased pEGFR (Y845, a Src-specific phosphorylation site), along with pSrc (Y416), in the drug-resistant lines, but not in the drug-sensitive lines (Figure 2B). Quantification of protein expression revealed the statistically significant positive association between phosphorylation status of ERK, Akt, mTOR, p70S6K, S6, EGFR, and Src and cixutumumab resistance (Figure 2B). RUs of cixutumumab-sensitive cells are as follows: pIGFR: 0.15 ± 0.07, 95% CI = 0.09 to 0.21, $P = .87$; pERK: 0.60 ± 0.08, 95% CI = 0.52 to 0.68, $P < .001$; pAkt: 0.87 ± 0.04, 95% CI = 0.83 to 0.91, $P < .001$; pmTOR: 0.85 ± 0.05, 95% CI = 0.8 to 0.9, $P < .001$; pp70S6K: 0.76 ± 0.15, 95% CI = 0.61 to 0.91, $P < .001$; pS6K: 0.83 ± 0.03, 95% CI = 0.8 to 0.86, $P < .001$; pEGFR (Y1068): 0.96 ± 0.08, 95% CI = 0.88 to 1.04, $P < .001$; pEGFR (Y845): 0.26 ± 0.11, 95% CI = 0.15 to 0.37, $P < .001$; pSrc: 0.28 ± 0.20, 95% CI = 0.08 to 0.48, $P < .001$.

IGF-Dependent Activation of the Integrin β3/Src Pathway Upon Cixutumumab Treatment

We monitored the kinetics of cixutumumab-induced signaling changes in 686LN cells. We found that Src, EGFR, Akt phosphorylation, and IGF-1R expression were time-dependently decreased by cixutumumab treatment in the absence of serum (Figure 3A and Supplementary Figure 6, available online). Conversely, Src and its downstream effectors that were initially dephosphorylated after 30 minutes of pretreatment with cixutumumab were immediately rephosphorylated in the presence of FBS or IGF-1 (Figure 3, A and B). IGF-1R remained dephosphorylated for 3 hours with no change in IGF-1R levels, whereas pSrc, pEGFR, and pAkt levels were rapidly restored at 1 hour and sustained up to 72 hours after treatment with cixutumumab. As Src is commonly activated by integrin signaling (17) and IGF-1 has the ability to directly bind to the specificity loop of integrin β3 (18), we hypothesized that Src could be activated via IGF-induced integrin signaling when IGF binding to IGF-1R is blocked by cixutumumab. We then assessed whether cixutumumab treatment changes IGF-dependent interaction between integrin β3 and intracellular proteins. Cixutumumab pretreatment increased FBS-induced associations between β3 and Src or p85α in a time-dependent manner and concurrent phosphorylation of FAK and Src in 686LN, FADU, and H226Br cells (Figure 3C and Supplementary Figure 7, available online), all of which were completely abolished by an IGF-1–neutralizing mAb (αIGF-1). Cells pretreated with cixutumumab for 1 hour also showed remarkable increases in association between integrin β3 and Src or p85α in response to IGF-1 stimulation (Figure 3D). The IGF-dependent interaction between IGF-1R and integrin β1 could have been mediated by scaffolding proteins such as RACK1, as previously suggested (26,27). IGF-1 treatment alone seemed to considerably enhance the associations between integrin β1 and Src or p85α. However, these associations were not obviously affected by cixutumumab treatment. Immunofluorescence staining also indicated that IGF-1 stimulation induced increases in Src and FAK phosphorylation that were further increased by cixutumumab treatment but completely abolished by coincubation with IGF-1 (αIGF-1) or integrin β3 (αβ3) neutralizing antibodies (Figure 3E and Supplementary Figure 8, available online). Consistent with the observations in cells cultured in UAPs, IGF-induced increases in pSrc and pFAK in 686LN cells attached to extracellular matrix remained unaffected by the cixutumumab treatment but were completely abolished by IGF-1 or integrin β3 neutralizing antibodies (Supplementary Figures 9 and 10, available online). We attempted to correlate expression levels of integrin αvβ3 at the cell surface with cixutumumab response. Immunofluorescence staining and quantification (Supplementary Figure 11, available online) and Western blot analysis (data not shown) of integrin αv and β3 expression at the cell surface revealed that integrin αv and β3 expression were not statistically significantly associated with cixutumumab sensitivity.

Binding of IGF to Integrin β3 and Activation of the Integrin–Src Signaling Cascade Upon Cixutumumab Treatment

We tested the hypothesis that IGF-I can directly activate integrin αvβ3. We first assessed whether addition of IGF-1 enhances the effects of known ligands of integrin β3, such as fibronectin (FN) or vitronectin (VN), on the activation of the integrin signaling cascade or whether IGF-1 alone can mimic the effect of a specific integrin ligand. As shown in Figure 4A, 686LN cells pretreated with cixutumumab showed an increased pSrc level following IGF-1 stimulation in a time-dependent manner. The pSrc expression level in 686LN cells was also increased in response to FN or VN. However, cixutumumab pretreatment did not induce detectable change in the ligand-induced pSrc level. Furthermore, the addition of IGF-1 showed no obvious increase in the FN- or VN-induced response in the cixutumumab-pretreated cells. These results suggest that integrin ligands, such as FN and VN, are not required for the IGF-1-induced activation of integrin signaling and that IGF-1 can mimic the effects of specific integrin ligands.

We next performed three different binding assays to obtain direct evidence for IGF binding to integrin β3 when its binding to IGF-1R is blocked by cixutumumab. The first cell adhesion analysis showed that small interfering RNA (siRNA) against IGF-1R or integrin β3 as single agents reduced H226Br cell adhesion to the immobilized IGF-1 (Figure 4B). The mean difference of cells treated with the two siRNAs (95% CI = 1.95 to 2.29) was statistically significantly greater than the sum of the mean difference of cells treated with IGF-1R (95% CI = 2.85 to 3.27) and that of cells treated with integrin β3 (95% CI = 3.66 to 4.16) siRNA alone ($P < .001$). H226Br and FADU cells transfected with integrin β1 siRNA showed moderately increased adhesion to the immobilized IGF-1 compared to control siRNA-transfected cells whereas both integrin β1- and control siRNA–transfected cells had reduced adhesion in the presence of cixutumumab (Supplementary Figure 12, available online). The second ligand blot assay showed robust binding of biotinylated IGF-1 to integrin β3, but not to integrin β1. Binding of biotinylated IGF-1 to integrin β3 was sequestered by IGF-1, verifying that

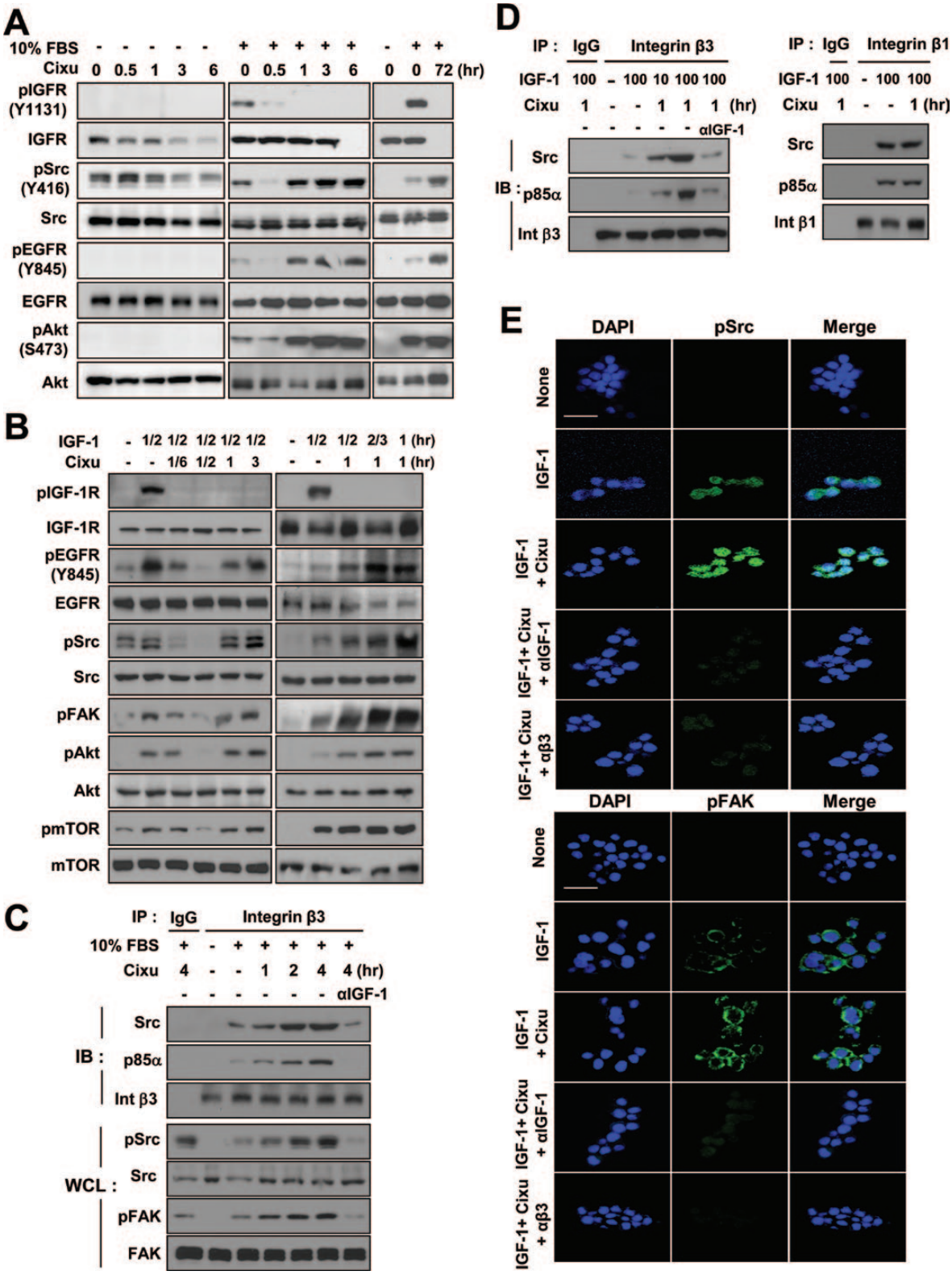

Figure 3. Insulin-like growth factor (IGF)–dependent activation of the β3 integrin/Src pathway upon cixutumumab (Cixu) treatment. **A and B**) 686LN cells grown in poly-(HEMA [poly-2-hydroxyethyl methacrylate])-coated plates (PCPs) were treated with cixutumumab (25 μg/mL) for indicated times prior to stimulation with 10% fetal bovine serum (FBS) for 30 minutes (**A**) or IGF-1 (100 ng/mL) for indicated times (**B**). Whole cell lysates (WCL) were analyzed by Western blotting for the indicated proteins. **C, D**) 686LN cells grown in PCPs were treated with cixutumumab (25 μg/mL) for indicated times prior to stimulation with 10% FBS (**C**) or IGF-1 (100 ng/mL) (**D**) in the absence or presence of anti-human IGF-1 neutralizing monoclonal antibodies (αIGF-1). Integrin β3 (**C, D**) or integrin β1 (**D**) immunoprecipitates (IP) were analyzed by Western blotting for the indicated proteins. Integrin β3 and β1 levels were also detected for IP from nonimmunized mouse serum (IgG). **E**) 686LN cells were treated with cixutumumab for 4 hour and further stimulated with IGF-1 in the absence or presence of anti–IGF-1 or anti–integrin β3 antibodies. Cells were paraffin-embedded and then subjected to immunofluorescence staining (magnification: ×630; scale bar: 20 μm). IB = immunoblot; Int β3: Integrin β3; Int β1: Integrin β1.

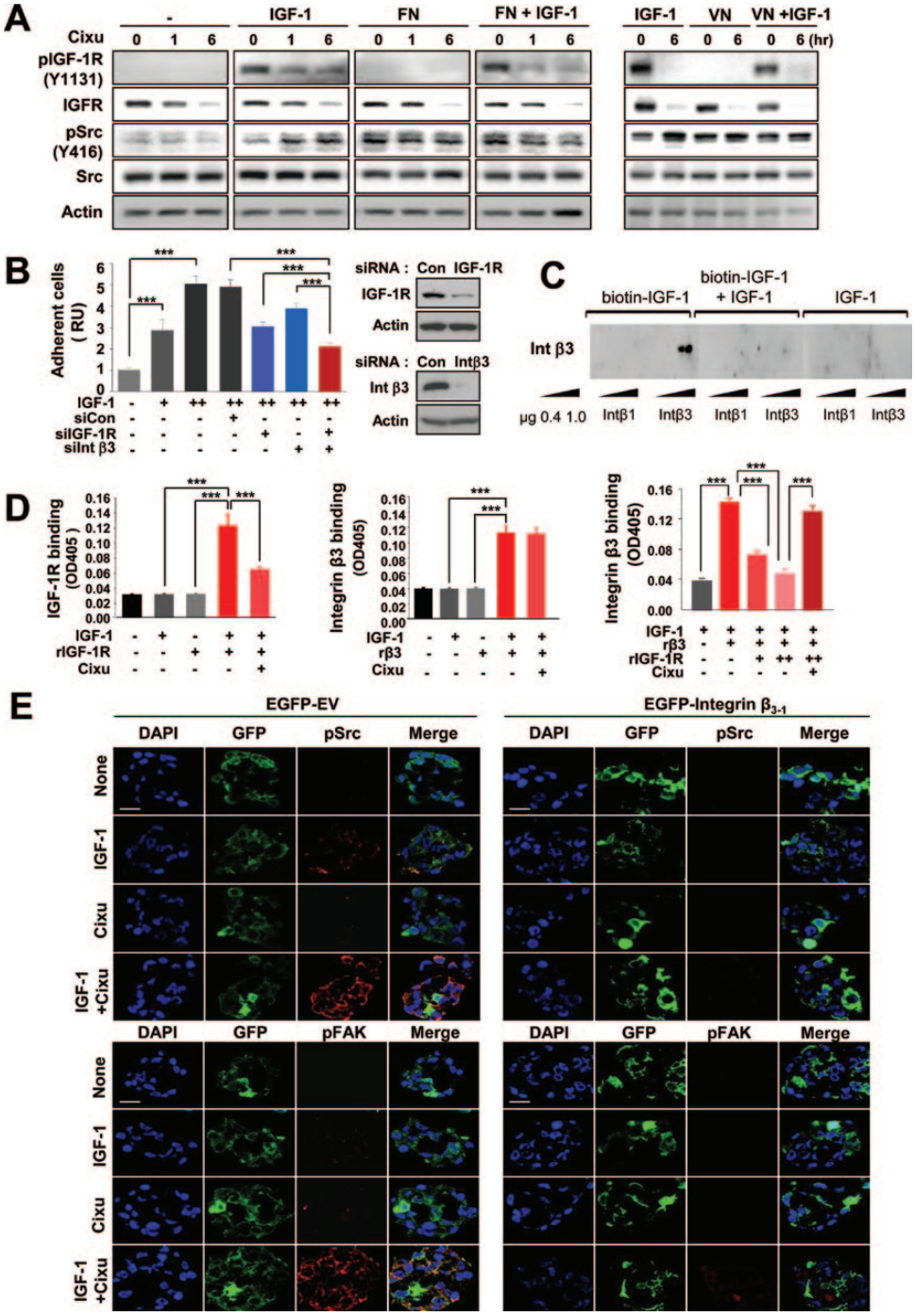

Figure 4. Activation of the integrin–Src signaling cascade through direct binding of IGF-1 to integrin β3. **A**) 686LN cells grown in poly-(HEMA [poly-2-hydroxyethyl methacrylate])-coated plates were treated with cixutumumab (Cixu; 25 μg/mL) for indicated times prior to stimulation with insulin-like growth factor 1 (IGF-1; 100 ng/mL), fibronectin (FN; 50 nM), vitronectin (VN; 25 nM), or their combination for 30 minutes as indicated. Whole cell lysates were analyzed by Western blotting for the indicated proteins. **B**) Adhesion of H226Br cells untransfected or transfected with scrambled siRNA (siCon), IGF-1R–specific, or integrin β3–specific siRNA to IGF-1 that was coated onto 96-well microtiter plates at 1 (+) or 2 (++) μg/mL coating concentrations. Data are presented as mean relative unit of cell adhesion ± SD (n = 6) of a representative data of at least two independent experiments. ***$P < .01$ by two-sided Student *t* test. Integrin β3 and IGF-1R levels after siRNA treatment were detected by Western blotting. **C**) Ligand blot analysis of integrin β3 and integrin β1 using biotinylated IGF-1. Recombinant integrin β3 (Intβ3) and integrin β1 (Intβ1) (0.4 and 1 μg) were resolved on polyacrylamide gels under nonreducing conditions and probed with biotinylated IGF-1 (200 ng/mL) in the absence or presence of IGF-1 (600 ng/mL). Avidin–horseradish peroxidase was added and the integrin β3 and integrin β1 were visualized using enhanced chemiluminescence. **D**) Ninety-six-well microtiter plates coated with IGF-1 were incubated with recombinant soluble IGF-1R (rIGF-1R; 5 μg/mL) or recombinant soluble Integrin β3 (rβ3; 5 μg/mL), alone or in combination, in the absence or presence of cixutumumab (25 μg/mL) for 2 hours. Bound IGF-1R (**left**) and integrin β3 (**middle and right**) were identified using anti–IGF-1R and anti-His monoclonal antibodies, respectively. The data are shown as the mean ± SD of a representative data set (n = 4) from at least two independent experiments; ***$P < .001$ by two-sided Student *t* test. **E**) FADU cells were transfected with empty or mutant integrin β3 expression vector (EGFP-β_{3-1}), and then treated with cixutumumab for 4 hours in the presence or absence of IGF-1. Expression of pSrc and pFAK was analyzed by immunofluorescence staining (magnification: ×630; scale bar: 20 μm). OD405 = absorbance at 405 nm; RU = relative unit.

IGF-1 was directly binding to integrin β3 (Figure 4C). The third ELISA assay also revealed statistically significant binding of rIGF-1R (0.120 ± 0.016, 95% CI = 0.10 to 0.14, $P < .001$; Figure 4D, left) and rβ3 (0.099 ± 0.007, 95% CI = 0.09 to 0.11, $P < .001$; Figure 4D, middle) to the IGF-1–coated plates. The rβ3 binding to the IGF-1–coated plates was suppressed by rIGF-1R in a dose-dependent manner; however, the rIGF-1R–induced ablation of IGF-1-rβ3 interaction was almost completely blocked by cixutumumab treatment (Figure 4D, right). An immunofluorescence analysis of FADU cells transfected with mutant integrin β3 (EGFP-$\beta_{3\text{-}1}$), in which the specificity loop of integrin β3 critical for IGF-1 binding is replaced with the corresponding sequence of integrin β1 (18,28), further showed that failure in IGF-1 binding to integrin β3 led to attenuation of cixutumumab-induced Src and FAK activation (Figure 4E). Collectively, these data suggest that, upon blockade of IGF binding to IGF-1R by cixutumumab treatment, IGF-1 binds to and activates integrin β3, but not to integrin β1, leading to FAK/Src-mediated stimulation of EGFR and PI3K/Akt.

Effect of Integrin β3/Src Signaling Inhibition on the Efficacy of Cixutumumab in Cixutumumab-Resistant HNSCC Cells

We attempted to test whether inactivation of integrin β3 or Src using a blocking antibody (αβ3) or an inhibitor (PP2) would prevent the IGF-dependent effects of cixutumumab on integrin/Src signaling and cell proliferation. Both cixutumumab-resistant (686LN and FADU) and cixutumumab-sensitive (OSC19) cells showed marked decreases in pSrc, pEGFR, and pAkt levels with no detectable changes in EGFR, Src, and Akt expression after 6 hours of treatment with αβ3 (10 μg/mL) (Supplementary Figure 13A, available online) or PP2 (10 μM) (Supplementary Figure 13B, available online). Treatment with αβ3 or PP2 almost completely blocked cixutumumab-induced increases in pSrc, pFAK, pEGFR, pAkt, and pmTOR in 686LN and FADU cells grown in PCPs (Figure 5A). In contrast, inactivation of β1 integrin by neutralizing antibody (αβ1) did not affect the cixutumumab-induced phosphorylation events in these cells (Figure 5B). Furthermore, the mean difference of viability of cixutumumab-resistant cells after treatment with cixutumumab and αβ3 (686LN: 95% CI = 0.26 to 0.38; FADU: 95% CI = 0.22 to 0.24; H226B: 95% CI = 0.21 to 0.29) was statistically significantly greater than the sum of mean differences in viability after treatment with cixutumumab (686LN: 95% CI = 0.85 to 0.97, $P < .001$; FADU: 95% CI = 0.76 to 0.86, $P < .001$; H226B: 95% CI = 0.68 to 0.92, $P < .001$) and that after treatment with αβ3 (686LN: 95% CI = 0.65 to 0.75, $P < .001$; FADU: 95% CI = 0.69 to 0.77, $P < .001$; H226B: 95% CI = 0.61 to 0.79, $P < .001$). In contrast, the combination regimens did not enhance the effects of cixutumumab on the viability of the cixutumumab-sensitive lines (OSC19 and UMSCC38) (Figure 5C). Treatment with PP2 also sensitized the drug-resistant, but not the drug-sensitive, lines to the cixutumumab treatment (Figure 5C). Specific blockade of Src through transfection with Src siRNA also blocked the IGF-dependent effects of cixutumumab on Src, FAK, Akt, and mTOR phosphorylation (Supplementary Figure 14A, available online) and statistically significantly augmented antiproliferative activities of the drug (Supplementary Figure 14B, available online) in 686LN and FADU cells. Treatment with adenoviruses expressing inhibitory c-Src tyrosine kinase (Ad-CSK) reduced cixutumumab-induced phosphorylation events in 686LN cells (Figure 5D). The mean difference in tumor volume with cixutumumab and Ad-CSK combination (95% CI = 107.12 to 329.88) was statistically significantly greater than the sum of mean differences in tumor volume for cixutumumab (95% CI = 563.1 to 976.5, $P < .01$) and tumor volume for Ad-CSK (95% CI = 302.1 to 564.1, $P < .05$) (Figure 5E). We also assessed the potential role of integrin-ERK activity in the cixutumumab resistance by assessing the benefit of cotargeting IGF-1R and ERK activity. However, we observed that a MEK inhibitor (PD98059) did not augment the antiproliferative effect of cixutumumab (Supplementary Figure 15, available online). These in vitro and in vivo results suggested that the inactivation of integrin/Src signaling overcome resistance to cixutumumab.

We finally assessed the benefit of integrin β3 or Src antagonism in the therapeutic efficacy of cixutumumab using tumors of HNSCC obtained from a human patient. In the primary cultured cells in PCPs, the mean difference of cell viability after treatment with cixutumumab and integrin β3 siRNA (siβ3 first combination: 95% CI = 0.32 to 0.38; siβ3 second combination: 95% CI = 0.42 to 0.54) were statistically significantly greater than the sum of mean differences in cell viability for cixutumumab (95% CI = 0.86 to 0.94; $P < .001$) and cell viability for each siRNA (siβ3 first combination: 95% CI = 0.68 to 0.8, $P < .001$; siβ3 second combination: 95% CI = 0.73 to 0.87; $P < .001$) (Figure 6A). The mean difference of cell viability after treatment with cixutumumab and a blocking antibody (αβ3) (95% CI = 0.22 to 0.30) or a Src inhibitor (PP2) (95% CI = 0.41 to 0.49) was also statistically significantly greater than the sum of mean differences in cell viability for cixutumumab (95% CI = 0.87 to 0.95; $P < .001$) and cell viability for αβ3 (95% CI = 0.65 to 0.77, $P < .001$) or PP2 (95% CI = 0.72 to 0.94; $P < .001$) (Figure 6A). The mean difference of apoptotic activity of cells cotreated with cixutumumab and αβ3 (95% CI = 5.46 to 5.78) or PP2 (95% CI = 4.24 to 4.72) was statistically significantly enhanced than the sum of apoptotic activity for αβ3 (95% CI = 2.15 to 2.41, $P < .001$) and apoptotic activity for PP2 (95% CI = 1.30 to 1.78, $P < .001$) (Figure 6B). To determine the in vivo benefit of inhibiting integrin β3 specifically, we employed liposome-encapsulated integrin β3 siRNA (29), cixutumumab, or both on the growth of a HNSCC patient-derived xenograft tumors. As predicted by the in vitro studies, a potent combinatory antitumor effect became apparent and statistically significant after the initiation of treatment and sustained over the course of the study (Figure 6C). At the end of the treatment, tumor volume of mice treated with cixutumumab and integrin β3 siRNA combination was 133.7 mm^3 (95% CI = 57.6 to 209.8 mm^3) statistically significantly smaller compared with that of mice treated with cixutumumab (1472.5 mm^3; 95% CI = 1150.7 to 1794.3 mm^3; $P < .001$) or integrin β3 siRNA (903.2 mm^3; 95% CI = 636.1 to 1170.3 mm^3; $P < .001$) alone. Cotreatment with cixutumumab and siβ3 induced markedly decreased pSrc levels and increased terminal deoxynucleotidyl transferase dUTP nick end labeling (TUNEL) staining in the tumors compared to the control or single-treatment groups (Figure 6D). Combination of cixutumumab with a clinically available Src inhibitor (dasatinib) also showed efficient regulation of the tumor growth (Figure 6E) and expression of pSrc and pAkt and TUNEL staining in the tumors (Figure 6F). These findings indicate the efficacy of cotargeting IGF-1R and integrin β3/Src signaling in the treatment of HNSCC in vivo.

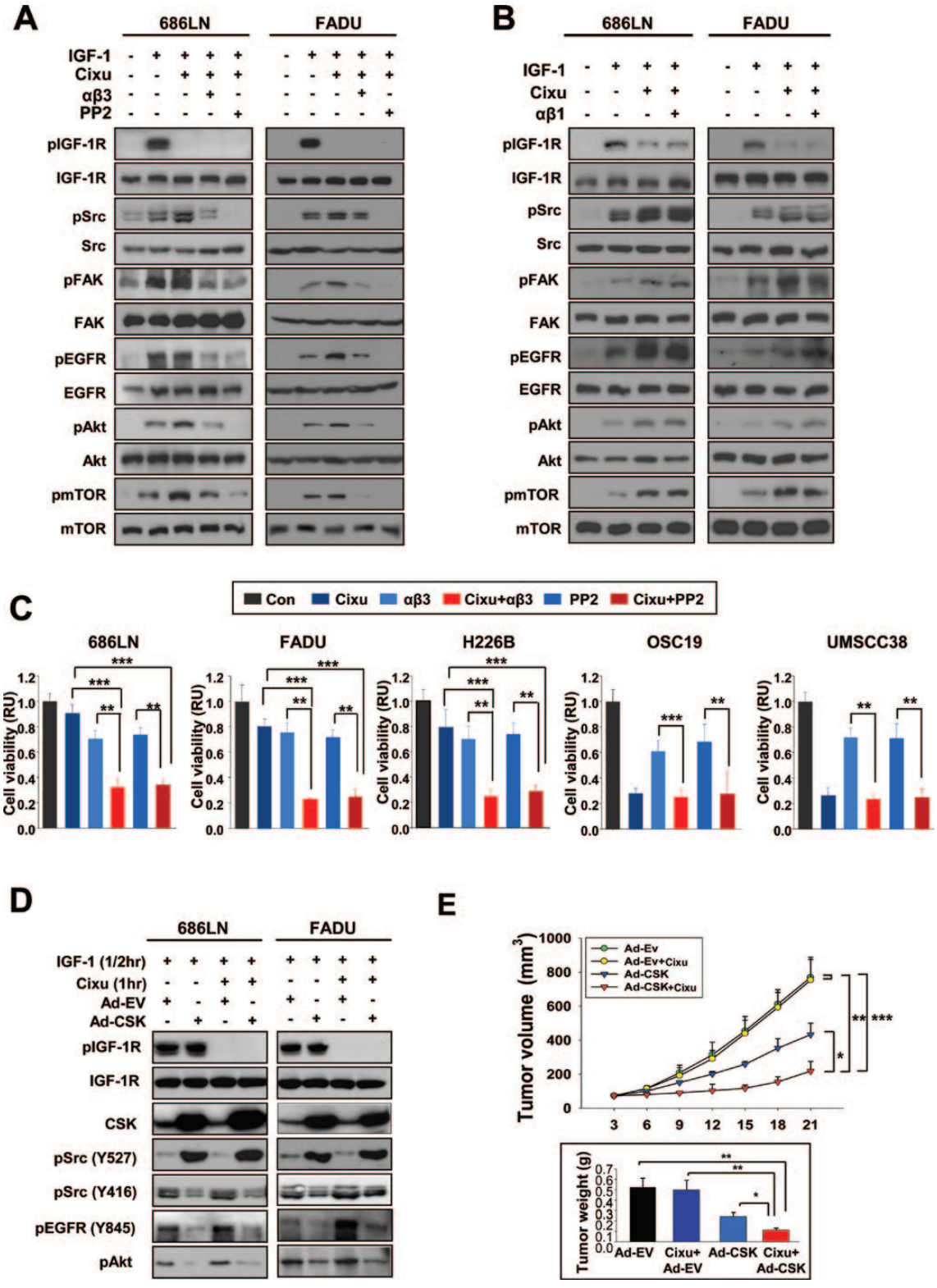

Figure 5. Effects of the integrin signaling inhibition on the cixutumumab (Cixu)–induced antiproliferative effects. **A, B, D**) 686LN and FADU cells grown in poly-(HEMA [poly-2-hydroxyethyl methacrylate])-coated plates (PCPs) were untreated or treated with cixutumumab (25 μg/mL), alone or in combination with anti-integrin β3 monoclonal antibody (mAb; 10 μg/mL), PP2 (10 μM) (**A**), anti-integrin β1 mAb (10 μg/mL) (**B**), Ad-EV or Ad-CSK (10 plaque-forming units [PFU]/cell) (**D**) for seven days prior to stimulation with insulin-like growth factor 1 (IGF-1; 100 ng/mL, 30 minutes). Western blot analysis was performed to detect the indicated proteins. **C**) Indicated cancer cells grown in PCPs were untreated (Con) or treated with cixutumumab (25 μg/mL), anti–integrin β3 mAb (αβ3, 10 μg/mL), PP2 (10 μM), or their combinations for seven days. Cell proliferation was analyzed by MTS assay. Each bar represents the mean value ± SD of six identical wells of a representative data set from at least two independent experiments. $^{**}P < .01$, $^{***}P < .001$ by two-sided Student *t* test. **E**) Preestablished 686LN tumor xenografts (n = 8) were injected with cixutumumab (Cixu; 25 mg/kg, intraperitoneal), Ad-EV (3×10^{11} PFU, intratumoral), Ad-CSK (3×10^{11} PFU, intratumoral), or their combination twice a week for indicated times. Bars represent mean ± SD; $^{*}P < .05$, $^{**}P < .01$, $^{***}P < .001$ by one-way analysis of variance. RU = relative unit.

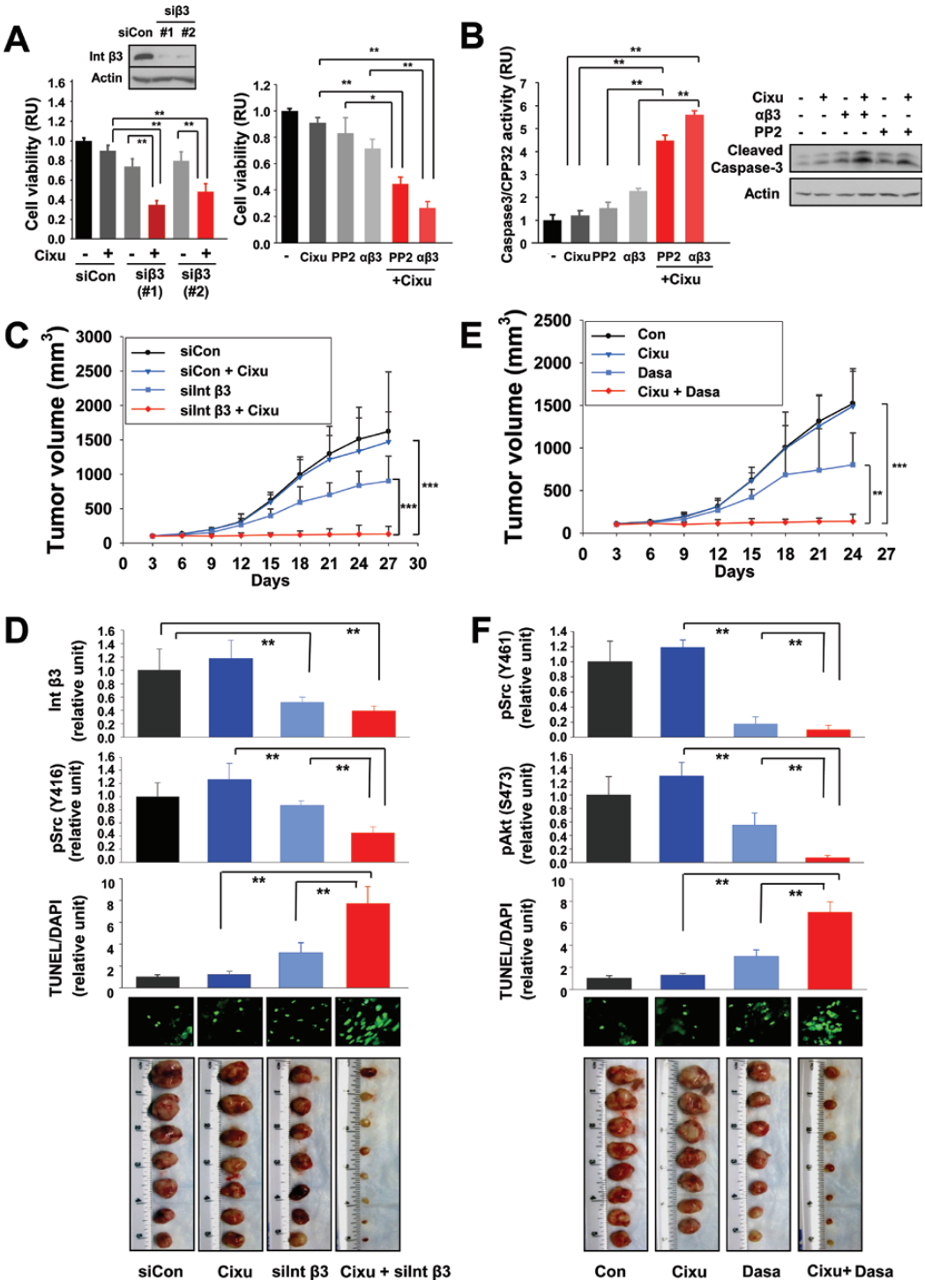

Figure 6. Effects of integrin β3 or Src blockade on antitumor effects of cixutumumab (Cixu) in head and neck squamous cell carcinoma (HNSCC) xenografts in vivo. **A, B**) Primary cultured cells from patients with HNSCC were transfected with either of two specific siRNAs (*1 or 2) against integrin β3 (siInt β3) or with control siRNA (siCon) (80 nM) for 24 hours (**A, left**). Suppression of integrin β3 expression by siRNA transfection was confirmed by Western blot analysis (**A, top**). Untransfected primary cultured cells were treated with cixutumumab (25 μg/mL), PP2 (10 μM), and integrin β3 monoclonal antibody (αβ3, 10 μg/mL) or their combinations for 72 hours (**A, right**). Cell viability was measured by MTS assay. The data are shown as the mean ± SD of seven identical wells of a representative data set of at least two independent experiments. $*P < .05$, $**P < .01$ by two-sided Student *t* test. The cell lysates (n = 4) were used for the caspase-3 colorimetric assay (**B, left**) and Western blot analysis (**B, right**). Bars represent mean ± SD. $**P < .01$ by two-sided Student *t* test. **C–F**) Athymic nude mice were transplanted with tumor tissue (2 mm^3) from HNSCC patients. Athymic nude mice with heterotransplants (n = 8) received siCon (5 μg intravenous twice weekly × 3), siCon and cixutumumab (Cixu; 10 mg/kg intraperitoneal, once weekly × 3), siIntegrin β3 (siInt β3; 5 μg intravenous, twice weekly × 3), and siIntegrin β3 and cixutumumab (**C, D**). Mice with each group (n = 8) received phosphate-buffered saline (Con), cixutumumab (Cixu), dasatinib (Dasa) (10 mg/kg, oral, daily), or cixutumumab and dasatinib (**E, F**). Data are presented as mean tumor volume ± SD for indicated times. $**P < .01$, $***P < .001$ by one way analysis of variance (C, E). Tumors were homogenized and subjected either to Western blot analysis for integrin β3 (Int β3), pSrc, or pAkt expression, and to TUNEL staining. Tumors in each group are shown (**D, F**). $**P < .01$ by two-sided Student *t* test. RU = relative unit.

Discussion

The present study elucidates a previously unrecognized role of integrin β3 in the inherent resistance to the anti–IGF-1R monoclonal antibody cixutumumab in HNSCC and NSCLC cells. Our study shows the following: 1) IGF-1, which failed to bind to IGF-1R due to the IGF-1R blockade by cixutumumab, bound to integrin β3 and induced concomitant activation of integrin signaling through FAK and Src and subsequent stimulation of EGFR and Akt. Under such conditions, the kinetics of cixutumumab's IGF-1R blockade paralleled the IGF-dependent stimulation of proximal and distal effectors of the integrin-Src signaling, including EGFR, PI3K/Akt, and FAK in cixutumumab-resistant cells. 2) Integrin β3 or Src antagonism was highly effective cixutumumab-mediated activation of integrin signaling in the antibody-resistant cells in vitro and in vivo. 3) Disruption of integrin β3 or Src restored proapoptotic activities of cixutumumab in vitro in drug-resistant cell lines as well as in vivo in nude mice bearing xenograft tumors of human HNSCC cell lines and in those bearing heterotransplant tumors from a patient with HNSCC (Figure 7). These results demonstrate the mechanistic insight for IGF-1R mAb resistance and provide a strong rationale for cotargeting IGF-1R and integrin β3/Src as an effective anticancer therapy in HNSCC and NSCLC.

Despite widespread enthusiasm about IGF-1R blockade for cancer therapy and a clear benefit observed in a small subset of patients treated with single-agent IGF-1R antagonists (8,9), the anticancer effects in advanced clinical trials have been ordinary and unsustained (10–12,30) through yet to be identified mechanisms of resistance. We also observed that a large number of human HNSCC and NSCLC cell lines were resistant to the IGF-1R–blocking mAb cixutumumab. This result is consistent with several preclinical studies showing only modest antiproliferative activities of IGF-1R–blocking mAbs in a variety of human cancer cells (31). Signaling through IR, PDGFRα, or AXL has been proposed to induce resistance against anti–IGF-1R therapies (22–25). However, we did not observe an obvious association between expression of these molecules and resistance to cixutumumab (data not shown). Given the interplay between the EGFR and IGF-1R pathways (32–36), resistance to cixutumumab could have been induced via switching to the EGFR/PI3K/Akt pathway. We found that cixutumumab treatment indeed triggered rapid phosphorylation of EGFR and Akt in cixutumumab-resistant cells. However, our subsequent study identified that EGFR and Akt are primarily, if not solely, activated as a result of activation of the integrin signaling cascades. These findings suggest complex cooperative loops in IGF-1R and integrin signalings. Indeed, IGF-1R blockade by

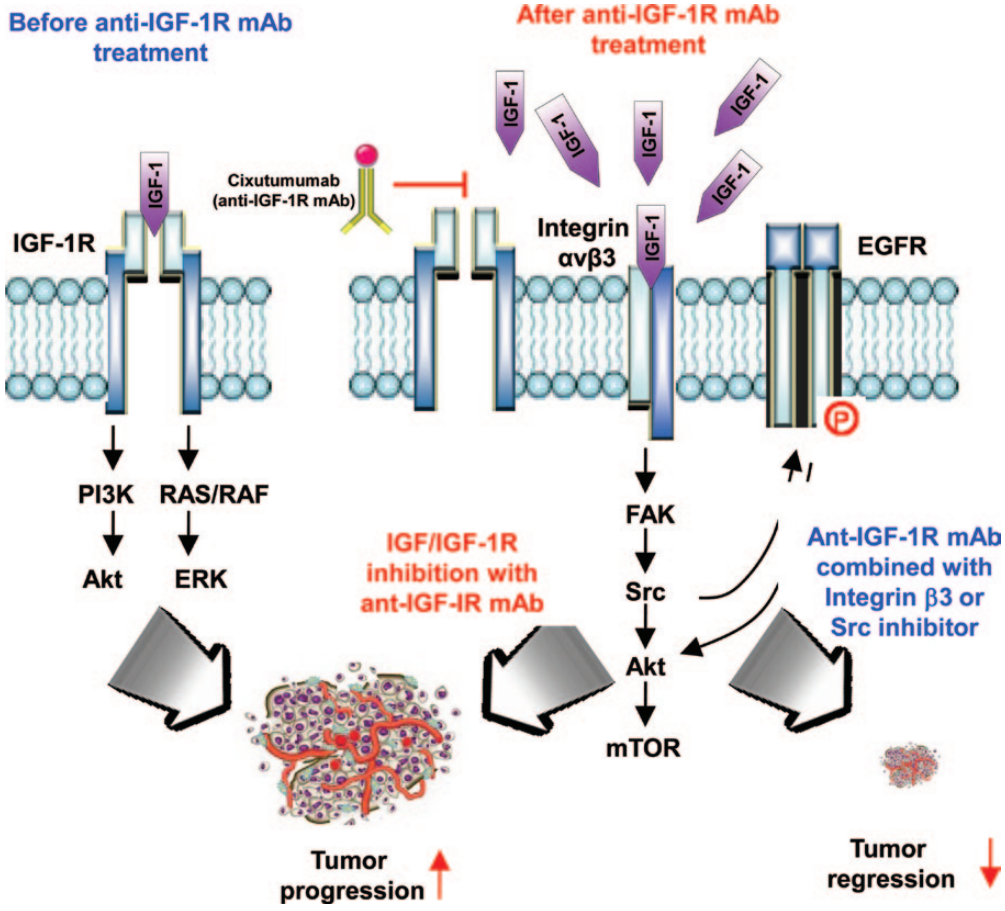

Figure 7. Schematic model of adaptive primary resistant responses by tumors to anti–IGF-1R monoclonal antibodies (mAbs). IGF/IGF-1R interaction stimulates downstream pathway with tumor progression. Tumors respond to IGF/IGF-1R pathway inhibition with anti–IGF-1R mAb, but mechanisms of primary resistance to the treatment are induced via alternative proliferative and survival signals through IGF/integrin β3 interaction and integrin-Src signaling cascade. Targeting integrin β3 or Src overcomes resistance to anti–IGF-1R mAbs. IGF-1R = insulin-like growth factor 1 receptor.

cixutumumab rescued the direct interaction between IGF-1 and integrin β3, which was hampered by soluble IGF-1R. Under that scenario, the IGF-mediated signaling would be redundant until the integrin-Src signaling becomes impaired by therapeutic intervention. Indeed, genomic and pharmacological approaches targeting β3 integrin or Src disrupted the IGF-dependent activities of cixutumumab in the integrin signaling and restored sensitivity to the growth inhibitory effects of cixutumumab in vitro and in vivo.

Our study has some limitations. First, it remains to be confirmed if activation of the integrin β3/Src signaling contributes to the anti–IGF-1R mAb resistance in clinical settings. Second, toxicology of combination regimens with integrin β3/Src and IGF-1R inhibitors is needed to determine their safety. Third, it is important to determine molecular changes that could serve as biomarkers for resistance to anti–IGF-1R mAb in clinical use.

In conclusion, this study identifies the IGF-induced integrin-Src signaling module as a novel mechanism of resistance against anti–IGF-1R mAb-based anticancer therapies in HNSCC and NSCLC. Although other mechanisms could be adopted by IGF-1R mAb-resistant tumors, our current study provides mechanistic insights into IGF-1R mAb resistance and potential strategies toward the reversal or prevention of the resistance. Considering that clinical development of integrin or Src inhibitors is ongoing (37–39), further clinical trials are warranted to test whether integrin β3 or Src blockade can effectively control resistance to IGF-1R mAb-based therapies.

References

1. Hanahan D, Weinberg RA. Hallmarks of cancer: the next generation. *Cell*. 2011;144:646–674.
2. Pollak MN. The insulin and insulin-like growth factor receptor family in neoplasia: an update. *Nat Rev Cancer*. 2012;12:159–169.
3. Bahr C, Groner B. The insulin like growth factor-1 receptor (IGF-1R) as a drug target: novel approaches to cancer therapy. *Growth Horm IGF Res*. 2004;14(4):287–295.
4. Garcia-Echeverria C. Medicinal chemistry approaches to target the kinase activity of IGF-1R. *IDrugs*. 2006;9(6):415–419.
5. Tolcher AW, Sarantopoulos J, Patnaik A, et al. Phase I, pharmacokinetic, and pharmacodynamic study of AMG 479, a fully human monoclonal antibody to insulin-like growth factor receptor 1. *J Clin Oncol*. 2009;27(34):5800–5807.
6. Olmos D, Postel-Vinay S, Molife LR, et al. Safety, pharmacokinetics, and preliminary activity of the anti-IGF-1R antibody figitumumab (CP-751,871) in patients with sarcoma and Ewing's sarcoma: a phase 1 expansion cohort study. *Lancet Oncol*. 2010;11(2):129–135.
7. Kurzrock R, Patnaik A, Aisner J, et al. A phase I study of weekly R1507, a human monoclonal antibody insulin-like growth factor-I receptor antagonist, in patients with advanced solid tumors. *Clin Cancer Res*. 2010;16(8):2458–2465.
8. Pappo AS, Patel S, Crowley J, et al. Activity of R1507, a monoclonal antibody to the insulin-like growth factor-1 receptor (IGF1R), in patients (pts) with recurrent or refractory Ewing's sarcoma family of tumors (ESFT): results of a phase II SARC study. *J Clin Oncol*. 2010;28:15s (suppl; abstr 10000).
9. Tap WD, Demetri GD, Barnette P, et al. AMG 479 in relapsed or refractory Ewing's family tumors (EFT) or desmoplastic small round cell tumors (DSRCT): phase II results. *J Clin Oncol*. 2010;28:15s (suppl; abstr 10001).
10. Patel S, Pappo J, Crowley J, et al. A SARC global collaborative phase II trial of R1507, a recombinant human monoclonal antibody to the insulin-like growth factor-1 receptor in patients with recurrent or refractory sarcomas. *J Clin Oncol*. 2009;27:15s (suppl; abstr 10001).
11. Reidy DL, Vakiani E, Fakih MG, et al. Randomized, phase II study of the insulin-like growth factor-1 receptor inhibitor IMC-A12, with or without cetuximab, in patients with cetuximab- or panitumumab-refractory metastatic colorectal cancer. *J Clin Oncol*. 2010;28(27):4240–4246.
12. Schmitz S, Kaminsky-Forrett MC, Henry S, et al. Phase II study of figitumumab in patients with recurrent and/or metastatic squamous cell carcinoma of the head and neck: clinical activity and molecular response (GORTEC 2008-02). *Ann Oncol*. 2012;23(8):2153–2161.
13. Hynes RO. Integrins: bidirectional, allosteric signaling machines. *Cell*. 2002;110(6):673–687.
14. Chen HC, Appeddu PA, Isoda H, Guan JL. Phosphorylation of tyrosine 397 in focal adhesion kinase is required for binding phosphatidylinositol 3-kinase. *J Biol Chem*. 1996;271(42):26329–26334.
15. Desgrosellier JS, Cheresh DA. Integrins in cancer: biological implications and therapeutic opportunities. *Nat Rev Cancer*. 2009;10(1):9–22.
16. Brozovic A, Majhen D, Roje V, et al. alpha(v)beta(3) Integrin-mediated drug resistance in human laryngeal carcinoma cells is caused by glutathione-dependent elimination of drug-induced reactive oxidative species. *Mol Pharmacol*. 2008;74(1):298–306.
17. Hood JD, Cheresh DA. Role of integrins in cell invasion and migration. *Nat Rev Cancer*. 2002;2(2):91–100.
18. Saegusa J, Yamaji S, Ieguchi K, et al. The direct binding of insulin-like growth factor-1 (IGF-1) to integrin alphavbeta3 is involved in IGF-1 signaling. *J Biol Chem*. 2009;284(36):24106–24114.
19. Rowinsky EK, Youssoufian H, Tonra JR, Solomon P, Burtrum D, Ludwig DL. IMC-A12, a human IgG_1 monoclonal antibody to the insulin-like growth factor I receptor. *Clin Cancer Res*. 2007;13(18):5549s–5555s.
20. Shin DH, Min HY, El-Naggar AK, et al. Akt/mTOR counteract the antitumor activities of cixutumumab, an anti-insulin-like growth factor I receptor monoclonal antibody. *Mol Cancer Ther*. 2011;10(12):2437–2448.
21. Mizushima H, Wang X, Miyamoto S, Mekada E. Integrin signal masks growth-promotion activity of HB-EGF in monolayer cell cultures. *J Cell Sci*. 2009;122(23):4277–4286.
22. Hendrickson AW, Haluska P. Resistance pathways relevant to insulin-like growth factor-1 receptor-targeted therapy. *Curr Opin Investig Drugs*. 2009;10:1032–1040.
23. Ulanet DB, Ludwig DL, Kahn CR, Hanahan D. Insulin receptor functionally enhances multistage tumor progression and conveys intrinsic resistance to IGF-1R targeted therapy. *Proc Natl Acad Sci U S A*. 2009;107(24):10791–10798.
24. Buck E, Eyzaguirre A, Rosenfeld-Franklin M, et al. Feedback mechanisms promote cooperativity for small molecule inhibitors of epidermal and insulin-like growth factor receptors. *Cancer Res*. 2008;68(20):8322–8332.
25. Huang F, Hurlburt W, Greer A, et al. Differential mechanisms of acquired resistance to insulin-like growth factor-I receptor antibody therapy or to a small-molecule inhibitor, BMS-754807, in a human rhabdomyosarcoma model. *Cancer Res*. 2010;70(18):7221–7231.
26. Hermanto U, Zong CS, Li W, Wang LH. RACK1, an insulin-like growth factor I (IGF-I) receptor-interacting protein, modulates IGF-I-dependent integrin signaling and promotes cell spreading and contact with extracellular matrix. *Mol Cell Biol*. 2002;22(7):2345–2365.
27. Kiely PA, O'Gorman D, Luong K, Ron D, O'Connor R. Insulin-like growth factor I controls a mutually exclusive association of RACK1 with protein phosphatase 2A and β1 integrin to promote cell migration. *Mol Cell Biol*. 2006;26(11):4041–4051.
28. Takagi J, Kamata T, Meredith J, Puzon-McLaughlin W, Takada Y. Changing ligand specificities of αvβ1 and αvβ3 integrins by swapping a short diverse sequence of the β subunit. *J Biol Chem*. 1997;272(32):19794–19800.
29. Verma A, Guha S, Diagaradjane P, et al. Therapeutic significance of elevated tissue transglutaminase expression in pancreatic cancer. *Clin Cancer Res*. 2008;14(8):2476–2483.
30. Karp DD, Paz-Ares LG, Novello S, et al. Phase II study of the anti-insulin-like growth factor type 1 receptor antibody CP-751,871 in combination with paclitaxel and carboplatin in previously untreated, locally advanced, or metastatic non-small-cell lung cancer. *J Clin Oncol*. 2009;27(15):2516–2522.
31. Gong Y, Yao E, Shen R, et al. High expression levels of total IGF-1R and sensitivity of NSCLC cells in vitro to an anti-IGF-1R antibody (R1507). *PLoS One*. 2009;4(10):e7273.
32. Morgillo F, Woo JK, Kim ES, Hong WK, Lee HY. Heterodimerization of insulin-like growth factor receptor/epidermal growth factor receptor

and induction of survivin expression counteract the antitumor action of erlotinib. *Cancer Res*. 2006;66(20):10100–10111.
33. Adams TE, McKern NM, Ward CW. Signaling by the type 1 insulin-like growth factor receptor: interplay with the epidermal growth factor receptor. *Growth Factors*. 2004;22(2):89–95.
34. Chakravarti A, Loeffler JS, Dyson NJ. Insulin-like growth factor receptor I mediates resistance to anti-epidermal growth factor receptor therapy in primary human glioblastoma cells through continued activation of phosphoinositide 3-kinase signaling. *Cancer Res*. 2002;62(1):200–207.
35. Liu B, Fang M, Lu Y, Mendelsohn J, Fan Z. Fibroblast growth factor and insulin-like growth factor differentially modulate the apoptosis and G1 arrest induced by anti-epidermal growth factor receptor monoclonal antibody. *Oncogene*. 2001;20(15):1913–1922.
36. Morgillo F, Kim WY, Kim ES, Ciardiello F, Hong WK, Lee HY. Implication of the insulin-like growth factor-IR pathway in the resistance of non-small cell lung cancer cells to treatment with gefitinib. *Clin Cancer Res*. 2007;13:2795–2803.
37. O'Donnell PH, Undevia SD, Stadler WM, et al. A phase I study of continuous infusion cilengitide in patients with solid tumors. *Invest New Drugs*. 2012;30:604–610.
38. Nabors LB, Mikkelsen T, Rosenfeld SS, et al. Phase I and correlative biology study of cilengitide in patients with recurrent malignant glioma. *J Clin Oncol*. 2007;25:1651–1657.
39. Zhang S,Yu D. Targeting Src family kinases in anti-cancer therapies: turning promise into triumph. *Trends Pharamcol Sci*. 2012;33:122–128.

Funding

This research was supported by the National Institutes of Health (grant R01 CA100816 to H.-Y. Lee) and by the National Research Foundation of Korea (grant funded by the Korea government, No. 2011-0017639 to H.-Y. Lee).

Affiliations of authors: Department of Thoracic/Head and Neck Medical Oncology (DHS, SPC, FMJ, SML, BSG) and Department of Experimental Therapeutics (KM), The University of Texas MD Anderson Cancer Center, Houston, TX; College of Pharmacy, Inje University, Gimhae, Gyungnam, Republic of Korea (H-JL); College of Pharmacy and Research Institute of Pharmaceutical Sciences, Seoul National University, Seoul, Republic of Korea (H-YM, M-SL, JWL, H-YL).